

Final Report - NEHRP

Award # 05HQGR0061

3D Modeling of Strong Ground Motion in the Pacific Northwest From Large (M8-9) Earthquakes in the Cascadia Subduction Zone

01 January 2005 – 30 June 2007

PI: Kim B. Olsen

Dept of Geological Sciences, San Diego State University, 5500 Campanile Dr, San Diego, CA 92182,

e-mail: kbolsen@sciences.sdsu.edu

Non-technical Summary

We have developed a model of seismic velocities and densities for the Pacific Northwest region from northern California to southern Canada and carried out the first 3D simulations of $M_w9.0$ and $M_w8.5$ megathrust earthquakes rupturing along the Cascadia subduction zone. Our simulations provide the first area-wide estimates of the ground motions to be expected from such an event, including the large urban areas of the Pacific Northwest, such as Vancouver, Seattle and Portland. Seattle experiences the largest long-period peak ground velocities while the values for Portland and Vancouver are smaller. Combined with an extended duration of the shaking of up to 5 minutes, generated by a combination of source and amplification effects in the 3D sedimentary basins, these long-period ground motions may inflict significant damage on the built environment, in particular on the highrises in downtown Seattle. Strain release in the Cascadia subduction zone by a series of $\sim M_w8.5$ events rather than a single $\sim M_w9.0$ megathrust earthquake would likely cause considerably less damage in the Pacific Northwest.

Abstract

We have developed a Community Velocity Model for the Pacific Northwest region from northern California to southern Canada and carried out the first 3D simulations of $M_w9.0$ and $M_w8.5$ megathrust earthquakes rupturing along the Cascadia subduction zone using a parallel supercomputer. Long-period ($<0.5\text{Hz}$) source models were designed by mapping the inversion results for the December 26, 2004 Sumatra-Andaman earthquake (Han et al 2006) onto the Cascadia subduction zone for the $M_w9.0$ scenarios and using pseudo-dynamic descriptions for the $M_w8.5$ scenarios. Our simulations provide the first area-wide estimates of the ground motions to be expected from such an event, including the large urban areas of the Pacific Northwest, such as Vancouver, Seattle and Portland. Seattle (41-116 cm/s) experiences the largest long-period peak ground velocities while the values for Portland (8-35 cm/s) and Vancouver (10-58 cm/s) are smaller. Combined with an extended duration of the shaking of up to 5 minutes, generated by a combination of source and amplification effects in the 3D sedimentary basins, these long-period ground motions may inflict significant damage on the built environment, in particular on the highrises in downtown Seattle. For the $M_w9.0$ events, a scenario with south-north rupture direction generated larger PGVs in Seattle and Vancouver metropolitan areas by about a factor of two, as compared to north-south rupture scenarios. The $M_w8.5$ scenarios generate PGVs (up to 10 cm/s in Seattle) 5-10 times smaller than those from $M_w9.0$ scenarios in the northern and central parts of the subduction zone. Scaling the rise times from the 2004 $M_w9.1-3$ Sumatra Andaman earthquake (mean=32s) to that predicted by the empirical relations by Somerville et al. (1999) (mean=14s) increases the PGVs by a factor of up to 2-3 at certain sites. We conclude that strain release in the Cascadia subduction zone by a series of $\sim M_w8.5$ events rather than a single $\sim M_w9.0$ megathrust earthquake would likely cause considerably less damage in the Pacific Northwest.

1. Introduction

Around 9:00 PM local time, on January 26th 1700, a giant earthquake struck the Pacific Northwest (approximately magnitude 9), caused by movement of the Juan de Fuca plate beneath the North American plate along the Cascadia subduction zone (see Figure 1) in the Pacific Northwest region (Ludwin et al 2005). The ~1000 km-long plate boundary poses one of the largest earthquake hazards in the Pacific Northwest region. Paleoseismic studies reveal a long history of large earthquakes (moment magnitudes larger than 8, hereafter referred to as megathrust events) with a recurrence period of approximately 500 years (Heaton and Hartzell, 1986; Atwater and Hemphill-Haley, 1997). No earthquake of such magnitude has occurred since the deployment of strong ground motion instruments in the Pacific Northwest, and a large uncertainty is associated with the ground motions expected from such an event. In addition, three major metropolitan areas are located in the model region, namely Seattle (3 million+ people), Vancouver (2 million+ people), and Portland (2 million+ people), all located above sedimentary basins prone to amplify the waves generated by a megathrust event. Therefore, it is imperative to estimate the level of ground motion to be expected in a future large subduction earthquake in the Pacific Northwest region. In this paper we present a 3D Community Velocity Model (CVM) for the Pacific Northwest region extending from southern Canada to northern California, and use the model to compute the first 3D simulations of M9.0 and M8.5 megathrust earthquakes nucleating in the Cascadia subduction zone.

2. Community Velocity Model (CVM) for the Pacific Northwest

Several ground motion modeling studies (e.g., Frankel and Stephenson, 2000; Pitarka et al 2004) have found strong basin effects for local earthquakes in the Seattle region, including basin-edge effects and amplification with basin depth. These studies show that a detailed 3D model of the Puget Sound Region is necessary to obtain realistic ground motions. In order to provide a model for estimation of ground motions, in particular for large megathrust earthquakes in the Cascadia subduction zone, we have developed a 3D CVM Version 1.3 of the crust and mantle in the Pacific Northwest (Stephenson, 2007). The areal extent of the model is shown in Figure 1.

The model consists of six geologic units: Continental sedimentary basins, continental crust, continental mantle, oceanic sediments, oceanic crust, and oceanic mantle. The Seattle fault represents the only other fault incorporated in the model, in addition to the Cascadia megathrust, due to its role as a seismogenic source in the Seattle Urban Hazards Maps (Frankel et al 2007). The Seattle fault trace was extracted from Blakely et al (2002) and projected to a depth of about 20 km assuming a 45° dip toward south. The P-wave velocity was derived for each unit from the available data. Except for the continental sedimentary basins, all densities and the S-wave velocities were then derived from the empirical relationship with P-wave velocity by Brocher (2005). The minimum and maximum densities were constrained to 2000 and 3500 kg/m³, respectively.

The continental sedimentary basins are subdivided into Quaternary and Tertiary geologic units. The thickness of the Quaternary deposits through the southern Puget Lowland was compiled by Jones (1996) and Johnson et al (1999) and used by Frankel and Stephenson (2000) for ground motion modeling in the Seattle basin. The data of Mosher and Johnson (2000) were incorporated to create the Quaternary-Tertiary interface in the Puget Lowland. A 1D profile of V_p was derived for the Quaternary deposits from land measurements and high-resolution marine seismic surveys (e.g., Williams et al 1999; Calvert et al 2003) with values of 1500 m/s, 1905 m/s and 1980 m/s at 0 m, 200 m and 1000 m depth, respectively. Quaternary V_s was then derived from V_{s30} and V_{p30} measurements by constraining the V_p/V_s ratio at the surface and 1 km depth to approximately 2.5 and 2.2, respectively.

The base of the Tertiary sediments within the Puget Lowland is inferred to be at the 4500 m/s isosurface, based on oil industry data (Brocher and Ruebel, 1998). This isosurface was extracted from the SHIPS (Seismic Hazards Investigation in Puget Sound) and 3D P-wave earthquake data tomography from Ramachandran et al (2006) that incorporates the same or similar data from many previous tomography studies in the Puget Lowland (e.g., Stanley et al 1999; Brocher et al 2001; Van Wagoner et al 2003). The

Willamette Valley basin deposits in the Portland area are derived from well data intersecting crystalline rocks under generally Tertiary deposits (Yeats et al 1996; Gannett et al 1998). Quaternary deposits are generally less than 30 m thick and are currently not included in the model. V_p of the Tertiary deposits in the Puget Lowland basins is based on tomography results from SHIPS and local earthquake data as calculated by Ramachandran et al (2006). A V_p depth structure similar to that of the Puget Lowland is assumed for the Willamette Valley, while V_s is estimated assuming a constant V_p/V_s ratio of 2.

The top of the continental crust below mean sea level was controlled by the smoothed continental shoreline as well as results of numerous published active and passive source studies along the continental margin (e.g., Trehu et al 1994; Clowes et al 1997; Flueh et al 1998; Fuis, 1998; Gulick et al 1998; Fleming and Trehu, 1999; Parsons et al 1999; Stanley and Villasenor, 2000; Bostock et al 2002; Ramachandran et al 2006). V_p is derived from the above-mentioned studies and, most prominently, from the 3D tomography model of Ramachandran et al (2006) through the Puget Lowland. The top surface of the continental mantle is derived from data of Chulick and Mooney (2002). We used the tomography of Stanley et al (1999) from the Puget Lowland area to constrain upper mantle V_p by extrapolating a generalized V_p -depth structure throughout the unit.

The ocean sediment unit represents accreted and sedimentary deposits overlying the top of the continental crustal unit and underlying the eastern portion of the bathymetric surface. V_p is derived from 3-D tomography results of Parsons et al (1999) and numerous active-source marine seismic surveys (e.g. Trehu et al 1994; Flueh et al 1998; Fuis, 1998; Gulick et al 1998; Fleming and Trehu, 1999). The top of the oceanic crustal unit is based on bathymetry and the results of Fluck et al (1997) and McCrory et al (2005) below the oceanic sediments, and is also defined to be the top of the Cascadia megathrust (subducting slab). Based on available marine-reflection data (e.g., Fuis, 1998) and studies from other parts of the world (e.g., Turcotte and Shubert, 1981) the thickness of the oceanic crust was set to 5 km. V_p was extrapolated from bulk values in marine seismic surveys (e.g., Trehu et al 1994; Flueh et al 1998; Fuis, 1998; Gulick et al 1998; Fleming and Trehu, 1999; Ramachandran et al 2006). Finally, the top of the oceanic mantle is derived by down-projecting the top of the oceanic crust 5 km and smoothing the resulting surface. V_p was set to vary from 7.9 km/s to 8.3 km/s between 10 km and 60 km depth, respectively.

An isosurface of a constant shear-wave velocity of 2500 m/s is shown in Figure 2. Notice the thick layer of oceanic sediments along the coast in the model, as well as the sedimentary basins in the Seattle and Vancouver areas. The E-W cross sections of the model in Figure 3 show the N-S variation in geometry of the Cascadia subduction zone, including the subducting slab. Surface topography is not included in the CVM V1.3.

3. Source Model for the Megathrust Scenarios

Since the most recent megathrust event in the Cascadia subduction zone dates back more than 300 years, no seismological data for such an event is available to constrain the earthquake rupture parameters specific to this area. Instead, we have used a source characterization derived from the December 26, 2004 M_w 9.1-9.3 Sumatra-Andaman earthquake which generated an unprecedented amount of seismic data. Specifically, we used an inversion result updated from Han et al (2006) (Chen Ji, Personal Communication, 2006).

The shape and extent of the Sumatra and Cascadia subduction zones are reasonably similar. However, some adjustments were necessary to map the results for the Sumatra-Andaman earthquake onto the Cascadia subduction zone. The slip inversion considered by Han et al (2006) approximated the rupture plane for the Sumatra-Andaman earthquake by 6 planes with dips of 6 - 8 1/4° for the shallow part and 15-25° for the deeper sections. The two northernmost planes, where limited moment release occurred (see Figure 4) were discarded due to the smaller area of the Cascadia subduction zone. The two southernmost rupture planes from the Sumatra-Andaman source inversion were translated and rotated to align with the strike (226°), dip and depth of the northernmost part of the Cascadia subduction zone with nucleation point in the deeper northern end. The two central rupture planes were translated and rotated to match the NS striking central and southern part of the subduction slab in the Cascadia model, with subfault dimensions of 4 km by 4 km.

The sources were then inserted into the uppermost part of the subduction slab dipping between 6° and 21° in the model area (see Figures 4 and 5). The slip distribution was scaled to a M_w 9.0 event and translated from the Sumatra-Andaman results in order to reflect this trend, assuming a rupture nucleation point at about 20 km depth (Figures 4-5). We simulated M_w 9.0 megathrust earthquakes with two different slip distributions (#1 and #2, generated by a lateral mirror image of #1 with some smaller adjustments, Figures 4-5) and two different rupture directions (north-south and south-north). The translation of the slip considered constraints from dislocation modeling and the thermal regime on the depth distribution of expected slip. In particular, the Cascadia subduction zone can be divided into a locked zone (\sim 4-12 km depth) and a transition zone (\sim 13-30 km depth) toward the east, with the majority of the slip expected to occur in the locked zone (Fluck et al 1997). The maximum and average slip for the M_w 9.0 scenario was 22 m and 6.3 m, respectively. The largest strain release occurs in the north-central part of the rupture zone for slip distribution #1, and in the south-central part of the rupture zone for slip distribution #2. The rupture initiation times were taken from the slip inversion and mapped into the Cascadia model (see Figure 6-7). The distribution of rupture initiation times from the source inversion generated an average rupture velocity of about 2.5 km/s, corresponding to 55-70% of the local shear-wave velocity on the Cascadia subduction slab.

We used the double triangle representation of sliprate functions as proposed by Graves and Pitarka (2004), with rise times obtained from the inversion for the Sumatra-Andaman earthquake. The mean and maximum rise times for the source were 32 s and 59 s, respectively. The mean rise time from the source inversion (Han et al., 2006) (\sim 32s) is much longer than that predicted by the empirical relation from Somerville et al. (1999) (14s), possibly due to limited resolution of the strong motion data used in the inversion. To address this uncertainty we estimate the effects on the ground motion by scaling the distributions of rise times by a constant factor, to obtain a mean value of 14 s. Finally, the rake was generated as a randomized distribution between 45° and 135° . Thus, our source description includes considerable complexity in all parameters, a requirement to ensure realistic ground motions in the surrounding areas. For example, Olsen et al (2007) found that the maximum PGVs in Los Angeles were reduced considerably using a source description for M_w 7.7 southern San Andreas fault scenarios with strong variation in rupture speed and pulse shape, as compared to those generated by a source with fixed pulse shape and constant rupture velocity (Olsen et al 2006).

Finally, it is possible that the slip deficit in the Cascadia subduction zone may be released by a series of smaller events, rather than by a single M_w \sim 9.0 earthquake. For this reason we also simulated two M_w 8.5 scenarios with the source description generated by the pseudo-dynamic method (Gattereri et al., 2004).

4. Numerical Modeling Parameters

The megathrust ground motion simulations were carried out using a 4th-order staggered-grid finite difference code (Olsen, 1994) with a coarse grained implementation of the memory variables for a constant-Q solid (Day and Bradley, 2001) and Q relations from Olsen et al (2003). The model dimensions are 1050 km along N-S, 550 km along E-W and 55 km along vertical, corresponding to 2200 by 4200 by 220 or approximately 2 billion grid points with a spatial resolution of 250m throughout the grid. The ocean water is included in the model, represented by $V_p=1500$ m/s, $V_s=0$ m/s and a density $\rho=1025$ kg/m³. We use the Cerjan et al (1985) absorbing boundary conditions and simulated 6.5 min of ground motion in the Pacific Northwest CVM for the megathrust event. The minimum velocity included in the computational model was 625 m/s due to computational limitations, only marginally higher than the minimum S-wave velocity of 600 m/s in the 3D Cascadia CVM V1.3. The simulation took about 40 wall clock hours on the 10 teraflops IBM Power4+ DataStar supercomputer at the San Diego Supercomputer Center (SDSC) using 1600 processors communicating via the message-passing interface (MPI).

5. Results

The peak ground velocities (PGVs) in the model area are shown in Figures 8-19. The maximum onshore

velocities are found along the coastline and generally subside eastward away from the subduction zone, with local amplification above the sedimentary basins, e.g., in the Seattle and Tacoma areas. In addition, the velocity seismograms predicted for the 5 most populous cities within the model extent (Vancouver, Seattle, Tacoma, Olympia and Portland) are shown, and their PGVs are listed in Table 1. Of the five urban areas, Seattle tends to experience the largest motions in the scenarios. The larger motion in Seattle, as compared to the other cities, is caused by a deeper underlying sedimentary basin (see Figure 2 for depths to the $V_s=2500$ m/s isosurface). In the following, we discuss the ground motions predicted for each of the scenarios.

M9.0 Scenario #1

The first scenario used slip distribution #1 and rupture time distribution #1 (nucleation in the northern end of the rupture zone). A map of PGVs and three-component synthetic seismograms at 5 selected sites are shown in Figures 8 and 9, respectively. The mean rise time is 32 s, as obtained from the inversion of the 2004 Sumatra-Andaman earthquake. The largest onshore PGVs (around 1 m/s) are obtained at the entrance of and just south of the Puget Sound. The largest PGV along E-W, N-S and vertical in Seattle, Tacoma, Olympia, Portland and Vancouver reach 41 cm/s, 19 cm/s, 15 cm/s, 8 cm/s and 10 cm/s, respectively. The duration of shaking is about 5 min at these sites.

M9.0 Scenario #2

This scenario used slip distribution #1 (generated as a lateral mirror image of slip distribution #1) and rupture time distribution #1 (nucleation in the northern end of the rupture zone). A map of PGVs and three-component synthetic seismograms at 5 selected sites are shown in Figures 10 and 11, respectively. The only change from scenario #1 is that mean rise time is 14 s, obtained by scaling the time times obtained from the inversion of the 2004 Sumatra-Andaman earthquake by a constant value according to the empirical relations by Somerville et al. (1999). The largest PGV along E-W, N-S and vertical in Seattle, Tacoma, Olympia, Portland and Vancouver reach 50 cm/s, 35 cm/s, 20 cm/s, 12 cm/s and 21 cm/s, respectively. The duration of shaking is about 5 min at these sites.

M9.0 Scenario #3

This scenario used slip distribution #2 and rupture time distribution #1 (nucleation in the northern end of the rupture zone). A map of PGVs and three-component synthetic seismograms at 5 selected sites are shown in Figures 12 and 13, respectively. The mean rise time is 14 s, obtained by scaling the time times obtained from the inversion of the 2004 Sumatra-Andaman earthquake by a constant value according to the empirical relations by Somerville et al. (1999). The largest PGV along E-W, N-S and vertical in Seattle, Tacoma, Olympia, Portland and Vancouver reach 50 cm/s, 36 cm/s, 21 cm/s, 28 cm/s and 29 cm/s, respectively. The duration of shaking is about 5 min at these sites.

M9.0 Scenario #4

This scenario used slip distribution #2 and rupture time distribution #2 (nucleation in the northern end of the rupture zone). A map of PGVs and three-component synthetic seismograms at 5 selected sites are shown in Figures 14 and 15, respectively. The mean rise time is 14 s, obtained by scaling the time times obtained from the inversion of the 2004 Sumatra-Andaman earthquake by a constant value according to the empirical relations by Somerville et al. (1999). This scenario generates the largest long-period ground motions in the Pacific Northwest region out of all simulated M9.0 events. The largest PGV along E-W, N-S and vertical in Seattle, Tacoma, Olympia, Portland and Vancouver reach 116 cm/s, 81 cm/s, 67 cm/s, 35 cm/s and 59 cm/s, respectively. The duration of shaking is about 5 min at these sites.

M8.5 Scenario #1

This scenario used slip, rupture times and rise times generated by the pseudo-dynamic method (Guatteri et al., 2004), with strain release in the northern part of the Cascadia subduction zone, see Figure 16. A map of PGVs and three-component synthetic seismograms at 5 selected sites are shown in Figures 16 and 17,

respectively. The largest PGV along E-W, N-S and vertical in Seattle, Tacoma, Olympia, Portland and Vancouver reach 12 cm/s, 9 cm/s, 5 cm/s, 5 cm/s and 2 cm/s, respectively. The duration of shaking is between 1 and 3 min at these sites.

M8.5 Scenario #2

This scenario used slip, rupture times and rise times generated by the pseudo-dynamic method (Gutteri et al., 2004), with strain release in the central part of the Cascadia subduction zone, see Figure 18. A map of PGVs and three-component synthetic seismograms at 5 selected sites are shown in Figures 18 and 19, respectively. The largest PGV along E-W, N-S and vertical in Seattle, Tacoma, Olympia, Portland and Vancouver reach 10 cm/s, 9 cm/s, 4 cm/s, 4 cm/s and 6 cm/s, respectively. Thus, the M8.5 scenario with strain release in the central part of the subduction zone generates larger PGV in Vancouver, but smaller PGV in Seattle, Olympia, Tacoma and Portland, as compared to the M8.5 scenario with strain release in the northern part of the subduction zone. The duration of shaking is between 1 and 3 min at these sites.

While the peak ground motions predicted in the larger cities in the Pacific Northwest for the megathrust earthquake are sufficiently large to cause damage on the built environment, particularly for Seattle, the extended duration of the ground motions poses an additional concern. Two-five minutes of long-period ground motions can be expected from the M9.0 scenarios, which may significantly weaken buildings. In particular, such duration of long period ground motion may be a problem for highrises, with the largest concentration in downtown Seattle. The Mw8.5 scenarios generate shorter durations of ground motion, between one and three minutes at the major metropolitans.

6. Discussion and conclusions

We have simulated wave propagation for M_w 9.0 and M_w 8.5 megathrust earthquakes nucleating in the Cascadia subduction zone in a new 3D CVM of the Pacific Northwest. The largest onshore long-period ground velocities are found along the coast, close to the largest asperities in the earthquake slip distribution. Our simulations provide the first area-wide estimates of the ground motions to be expected from such an event, including the large urban areas of the Pacific Northwest, such as Vancouver, Seattle and Portland. Seattle experiences the largest long-period peak ground velocities (41-116 cm/s), while the values for Portland (8-35 cm/s) and Vancouver (10-58 cm/s) are much smaller. Combined with an extended duration of the shaking of up to 5 minutes, generated by a combination of source and amplification effects in the 3D sedimentary basins, these long-period ground motions may inflict significant damage on the built environment, in particular on the highrises in downtown Seattle. For the M_w 9.0 events, scenarios with south-north rupture direction (up to ~100 cm/s in Seattle) tend to generate larger PGVs in Seattle and Vancouver metropolitan areas by about a factor of two, as compared to north-south rupture scenarios.

Scaling the rise times from the 2004 M_w 9.1-3 Sumatra Andaman earthquake (mean=32s) to that predicted by the empirical relations by Somerville et al. (1999) (mean=14s) increases the PGVs by a factor of up to 2-3 at certain sites. The M9 scenarios generate PGVs generally an order of magnitude larger than those from M8.5 (up to 12 cm/s in Seattle) scenarios in the northern and central parts of the subduction zone.

The resolution of the velocity model for the Pacific Northwest varies strongly within the area considered in this study. The urbanized regions, in particular the sedimentary basins in the Puget Lowland, are generally well constrained. However, other parts of the model, in particular the southern part of the model where constraints from data are sparse, contain larger uncertainties. For example, little or no information was available to construct the velocity model for most onshore areas south of Olympia, and near-surface shear-wave velocities are likely overestimated (see Figure 2). Parts of the CVM have already been validated against recorded data (Frankel and Stephenson, 2000; Pitarka et al 2004), and additional validation of the 3D velocity model of the Cascadia subduction zone should be carried out in future studies. Such validation studies should also target the relations for Q_p and Q_s used in this study (Olsen et al 2003).

Despite these limitations and uncertainties of the CVM and ground motion estimates, our results indicate that the societal impact of a megathrust earthquake in the Pacific Northwest will be enormous. Long-period PGVs of 10's of cm/s in Seattle and surrounding areas (possibly much higher if the rise times obtained from the Sumatra-Andaman are indeed too long) are bound to cause widespread damage, particularly for the highrises in the area. Additional megathrust scenarios should be simulated in the future to more accurately assess the impact on man-made structures and population of the Pacific Northwest.

Acknowledgements

This work was supported through DOI U.S. Geological Survey # 05HQGR0061 and the Southern California Earthquake Center (SCEC). SCEC is funded through the NSF cooperative agreement EAR-8920136 and USGS Cooperative Agreements 14-08-0001-A0899 and 1434-HQ-97AG01718. The simulation was carried out on the IBM Teraflop DataStar parallel computer at San Diego Supercomputer Center (SDSU). The 3D velocity model was developed by Bill Stephenson, of the USGS, Golden Colorado. Martin Mai, of the ETH in Zurich, Switzerland, generated the pseudo-dynamic source for the Mw8.5 scenarios. Andreas Geisselmeyer, Ulm University, Germany, helped map the source description for the Mw9.0 scenarios from the 2004 Sumatra-Andaman earthquake onto the Cascadia subduction zone.

Publications derived from this project

Olsen, K.B., W.J. Stephenson, and A. Geisselmeyer (2008). 3D Crustal Structure and Long-period Ground Motions From a M9.0 Megathrust Earthquake in the Pacific Northwest Region, *Jour. Seismol.*, 2008-2, in press.

Olsen, K.B., A. Geisselmeyer, and W.J. Stephenson (2007). 3D modeling of ground motion in the Pacific Northwest from large earthquakes in the Cascadia subduction zone, *Seism. Res. Lett* **78**, 273.

Olsen, K.B., A. Geisselmeyer, W.J. Stephenson, and P.M. Mai (2007). 3D modeling of ground motion in the Pacific Northwest from large earthquakes in the Cascadia subduction zone, *EOS, Trans. AGU* 88(52), *Fall Meet. Suppl.* S31B-0451.

References

- Atwater BF, Hemphill-Haley E (1997) Recurrence intervals for Great earthquakes of the past 3,500 years at northwestern Willapa Bay, Washington, U.S. Geological Survey Professional Paper 1576, Washington D.C., United States Government Printing Office, 108 pp.
- Blakely RJ, Wells RE, Weaver CSS, Johnson SY (2002) Location, structure, and seismicity of the Seattle fault zone, Washington: Evidence from aeromagnetic anomalies, geologic mapping, and seismic-reflection data, *Geol. Soc. Am. Bull.*, 114, 169-177.
- Bostock MG, Hyndman RD, Rondenay S, Peacock SM (2002). An inverted continental Moho and serpentinization of the forearc mantle, *Nature* **417**, 536-538.
- Brocher TM (2005). Empirical relations between elastic wavespeeds and density in the earth's crust, *Bull. Seis. Soc. Am.* **95**, 2081-2092.
- Brocher T, Parsons T, Blakeley RJ, Christensen NI, Fisher MA, Wells RE, and the SHIPS working group (2001) Upper crustal structure in Puget Lowland, Washington: results from the 1998 seismic hazards investigation in Puget Sound, *J. Geophys. Res.* 106-B7: 13541-13564.
- Brocher T, Ruebel AL (1998) Compilation of 29 sonic and density logs from 23 oil test wells in western Washington state, U.S. Geological Survey, Open File Report.
- Calvert AJ, Fisher MA, Johnson SY, Brocher TM, Creager KC, Crosson, RS, Hyndman RD, Miller, KC, Mosher D, Parsons, R, Pratt TL, Spence G, Brink U ten, Trehu AM, Weaver CS (2003) Along-strike variations in the shallow seismic velocity structure of the Seattle fault zone; evidence for fault segmentation beneath Puget Sound, *J. Geophys. Res.* **108**, doi: 10.1029/2001JB001703.
- Cerjan C, Kosloff D, Kosloff R, Reshef M (1985) Absorbing boundary conditions for acoustic and elastic wave equations, *Bull. Seis. Soc. Am.* **67**, 1529-1540.
- Chulick GS, Mooney WD (2002) Seismic structure of the crust and uppermost mantle of North America and adjacent oceanic basins: a synthesis, *Bull. Seis. Soc. Am.* **92**, 2478-2492.

- Clowes RM, Baird DJ, Dehler SA (1997) Crustal structure of the Cascadia subduction zone, southwestern British Columbia, from potential field and seismic studies, *Can J. Earth Sci* **34**, 317-335.
- Day SM, Bradley CR (2001) Memory-efficient simulation of anelastic wave propagation, *Bull. Seism. Soc. Am.* **91**, 520-531.
- Fleming SW, Trehu AM (1999) Crustal structure beneath the central Oregon convergent margin from potential field modeling: evidence for a buried basement ridge in local contact with a seaward dipping backstop, *J. Geophys. Res.* **104**, B9, 20431-20447.
- Fluck P, Hyndman RD, Wang K (1997) Three-dimensional dislocation model for great earthquakes of the Cascadia subduction zone, *J. Geophys. Res.* 102-B9:20539-20550.
- Flueh E.R, Fisher MA, Bials J, Childs JR, Klaeschen D, Kukowski N, Parsons T, Scholl DW, Brink U ten, Trehu AM, Vidal N (1998) New seismic images of the Cascadia subduction zone from cruise SO108-ORWELL, *Tectonophysics* **293**, 69-84.
- Frankel A, Stephenson WJ (2000) Three-dimensional simulations of ground motions in the Seattle region of earthquakes in the Seattle fault zone, *Bull. Seis. Soc. Am.* **90**, 1251-1267.
- Frankel AD, Stephenson WJ, Carver DL, Williams RA, Odom JK, Rhea S (2007) Seismic hazard maps for Seattle incorporating 3D sedimentary basin effects, nonlinear site response, and rupture directivity, U.S. Geological Survey Open File Report 2007-1175, 77 p., 3 pls.
- Fuis GS (1998) West margin of North America – a synthesis of recent seismic transects, *Tectonophysics* **288**, 265-292.
- Gannett MW, Caldwell RR (1998) Geologic framework of the Willamette Lowland aquifer system, Oregon and Washington, USGS Prof. Paper 1424-A, 32p, 8 plates.
- Graves RW, Pitarka A (2004) Broadband time history simulation using a hybrid approach, *Proceedings of the 13th World Conference on Earthquake Engineering*, Vancouver, B,C, Canada, Paper No. 1098.
- Guatteri, M., P.M. Mai, and G.C. Beroza (2004). A pseudo-dynamic approximation to dynamic rupture models for strong ground motion prediction, *Bull. Seis. Soc. Am.*, Vol 94 (6), pp. 2051-2063.
- Gulick SPS, Meltzer AM, Clarke SH (1998). Seismic structure of the southern Cascadia subduction zone and accretionary prism north of the Mendocino triple junction, *J. Geophys. Res.*, **103**, B11, 27207–27222.
- Han, S-C., C.K. Shum, M. Bevis, C. Ji, and C-Y. Kuo (2006). Crustal dilatation observed by GRACE after the 2004 Sumatra-Andaman earthquake, *Science* **313**, no 5787, 658-662, DOI 10.1126/Science.1128661.
- Heaton T, Hartzell S (1986) Source characteristic of hypothetical subduction earthquakes in the northwestern United States, *Bull. Seis. Soc. Am.* **76**, 675-708.
- Ji C, Helmberger DV, Wald DJ, Ma KF (2003) Slip history and dynamic implications of the 1999 Chi-Chi, Taiwan, earthquake, *Journal of Geophysical Research-Solid Earth*, **108** (B9), art. no.-2412.
- Johnson, SY, Dadisman SV, Childs JR, Stanley WD (1999) Active tectonics of the Seattle fault and central Puget Sound, Washington—implications for earthquake hazards, *Geol. Soc. Am. Bull.*, **111**, 1042–1053.
- Jones MA (1996) Thickness of unconsolidated deposits in the Puget Sound Lowland, Washington and British Columbia, Water-Resources Investigations - U. S. Geol. Surv. Report: WRI 94-4133, 1 sheet.
- Ludwin RS, Dennis R, Carver D, McMillan AD, Losey R, Clague J, Jonientz-Trisler C, Bowe chop J, Wray J, and James K (2005) Dating the 1700 Cascadia earthquake: Great coastal earthquakes in native stories, *Seism. Res. Lett.* **76**, 140-148.
- McCrory PA, Blair JL, Oppenheimer, DH. and Walter SR (2005) Depth to the Juan de Fuca Slab Beneath the Cascadia Subduction Margin— A 3-D Model for Sorting Earthquakes, U.S. Geological Survey Data Series 91.
- Mosher DC, Johnson SY (2000) Juan de Fuca Atlas—Neotectonics of the Eastern Juan de Fuca Strait: a digital geological and geophysical atlas, Geological Survey of Canada OF #3931.
- Parsons T, Wells RE, Fisher MA, Flueh E, Brink ten U (1999) Three-dimensional velocity structure of Siletzia and other accreted terranes in the Cascadia forearc of Washington, *J. Geophys. Res.*, **104**, n. B8, p. 18015–18039.
- Olsen KB (1994) Simulation of three-dimensional wave propagation in the Salt Lake Basin, *Ph.D. Thesis*, University of Utah, Salt Lake City, Utah, 157 p.
- Olsen KB, Day SM, Bradley CR (2003) Estimation of Q for long-period (>2 s) waves in the Los Angeles Basin, *Bull. Seis. Soc. Am.* **93**, 627-638.
- Olsen KB, Day SM, Minster JB, Cui Y, Chourasia A, Faerman M, Moore R, Maechling P, Jordan T (2006) Strong shaking in Los Angeles expected from southern San Andreas earthquake, *GRL* **33**, L07305, doi:10.1029/2005GL025472.
- Olsen KB, Day SM, Minster JB, Cui Y, Chourasia A, Okaya D, Maechling P, Jordan T (2006) TeraShake 2: simulation of Mw 7.7 earthquakes on the southern San Andreas fault with spontaneous rupture description, *Bull. Seis. Soc. Am.*, in review.
- Olsen, KB, W.J. Stephenson, and A. Geisselmeyer (2008). 3D Crustal Structure and Long-period Ground Motions From a M9.0 Megathrust Earthquake in the Pacific Northwest Region, *Jour. Seismol.*, in press.
- Pitarka A, Graves R, Somerville P (2004) Validation of a 3D velocity model of the Puget Sound Region based on modeling ground motion from the 28 February 2001, Nisqually earthquake, *Bull. Seis. Soc. Am.* **94**, 1670-1689.
- Ramachandran K, Hyndman RD, Brocher TM (2006) Regional P-wave velocity structure of the northern Cascadia subduction zone,

Jour. Geophys. Res. **111**, B12, B12,301, doi:1.1029/2005JB004108.

Somerville P, Irikura K, Graves R, Sawada S, Wald D, Abrahamson N, Iwasaki Y, Kagawa T, Smith N, Kowada A (1999) Characterizing crustal earthquake slip models for the prediction of strong ground motion, *SRL* **70**, 59-80.

Stanley D, Villasenor A 2000 Models of downdip frictional coupling for the Cascadia megathrust, *Geophys. Res. Lett.* **27**, n. 10, 1551–1554.

Stanley D, Villasenor A, Benz H (1999) Subduction zone and crustal dynamics of western Washington: A tectonic model for earthquake hazards evaluation, USGS OF 99-311, <http://pubs.usgs.gov/of/1999/of-99-0311>.

Stephenson WJ (2007) Velocity and density models incorporating the Cascadia subduction zone for 3-D ground motion simulations, U.S. Geological Survey Open File Report, 28 pp.

Turcotte DL, Schubert G (1982) *Geodynamics: Applications of continuum Physics to Geological problems*, John Wiley & Sons, p. 12.

Trehu AM, Asudeh I, Brocher TM, Luetgert JH, Mooney WD, Nabelek JL, Nakamura Y (1994). Crustal architecture of the Cascadia forearc, *Science*, **266**, 237–242.

Van Wagoner TM, Crosson RS, Creager KC, Medema G, Preston L, Symons NP, Brocher TM (2002) Crustal structure and relocated earthquakes in the Puget Lowland, Washington, from high-resolution seismic tomography, *J. Geophys. Res.*, **107**, doi: 10.1029/2001JB000710.

Williams RA, Stephenson WJ, Frankel AD, Odum JK (1999) Surface seismic measurements of near-surface P- and S-wave seismic velocities at earthquake recording stations, Seattle, Washington, *Earthquake Spectra*, **15**, n. 3, 565–584.

Yeats R.S, Graven EP, Werner KS, Goldfinger C, Popowski TA (1996) *Tectonics of the Willamette Valley, Oregon*, Rogers, A.M., Walsh, T.J., Kockelman, W.J., and Priest, G.R. (editors), *Assessing earthquake hazards and reducing risk in the Pacific Northwest*; Volume 1, P 1560, 183-222.

Table 1. Peak ground velocities (cm/s) predicted in 5 major cities of the Pacific Northwest

Scenario	Comp.	Olympia	Tacoma	Seattle	Portland	Vancouver
	E-W	4.3	9.4	11.9	5.1	2.4
M85 (North)	N-S	5.2	7.4	7.6	3.5	1.7
	Vertical	3.4	3.0	5.9	3.8	1.4
	E-W	3.7	6.9	7.7	3.0	3.7
M85 (Center)	N-S	3.5	8.9	1.1	1.2	6.0
	Vertical	4.1	2.3	9.9	3.9	3.7
	E-W	10.4	18.8	35.0	8.0	9.6
M9 #1	N-S	14.6	15.2	41.1	3.8	8.3
	Vertical	8.8	11.2	11.9	7.9	5.6
	E-W	14.1	29.6	38.6	11.6	20.6
M9 #2	N-S	20.4	35.1	50.2	6.2	15.0
	Vertical	16.7	15.9	23.6	11.1	10.0
	E-W	12.0	33.8	46.1	11.7	29.0
M9 #3	N-S	13.4	36.2	49.9	9.1	17.6
	Vertical	20.7	23.2	36.6	27.9	16.5
	E-W	66.6	81.4	115.5	23.7	58.3
M9 #4	N-S	47.3	73.9	88.6	24.5	56.4
	Vertical	42.0	34.0	87.5	34.8	32.1

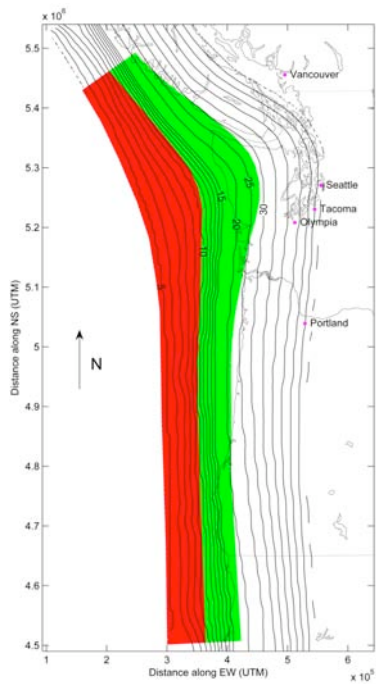


Figure 1. The subduction slab in the Cascadia area (contours in kilometers below sealevel. Red and green colors depict estimates of the locked and transition zones, respectively, from Fluck et al (1997).

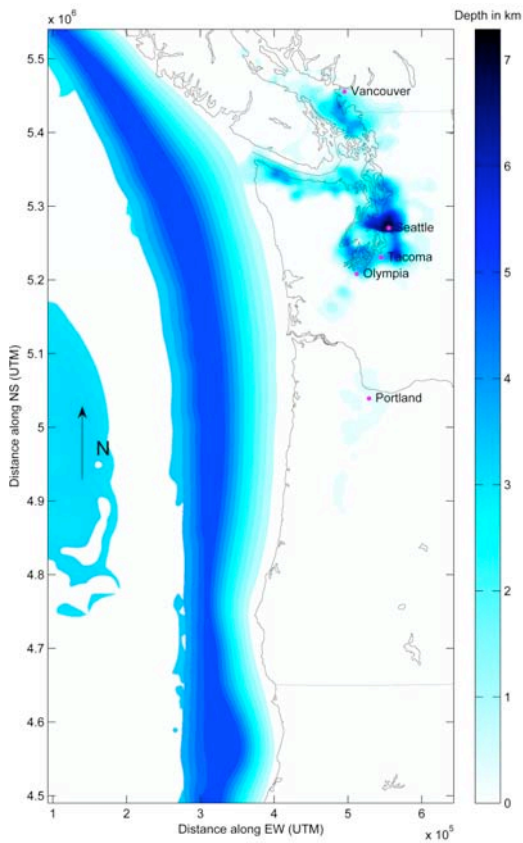


Figure 2. Isosurface of a shear-wave velocity of 2500 m/s in the Cascadia 3D CVM V1.3.

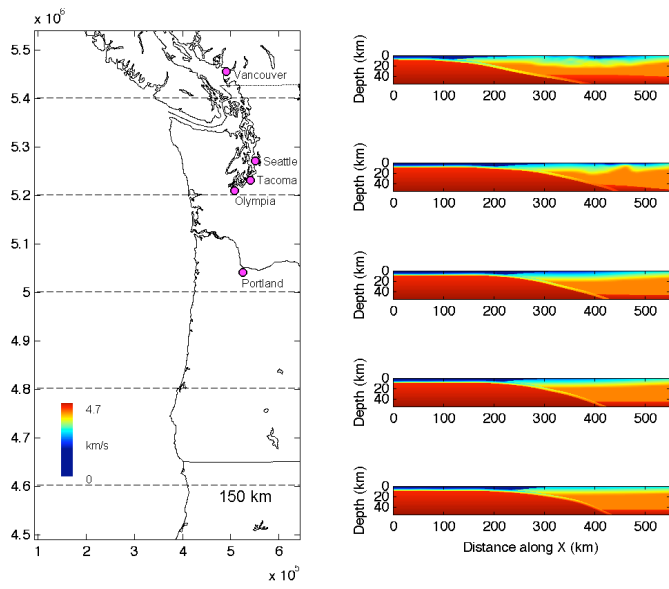


Figure 3. Cross sections of the S-wave velocity (right) along 5 E-W profiles (left) in the Pacific Northwest CVM V1.3.

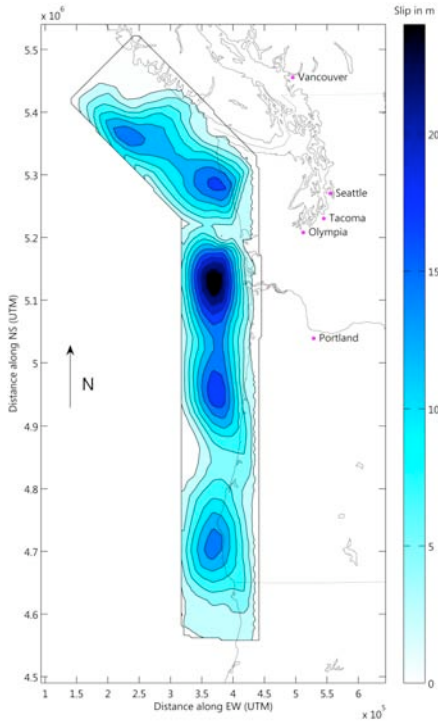


Figure 4. Slip distribution #1 used in the Cascadia megathrust scenario simulation.

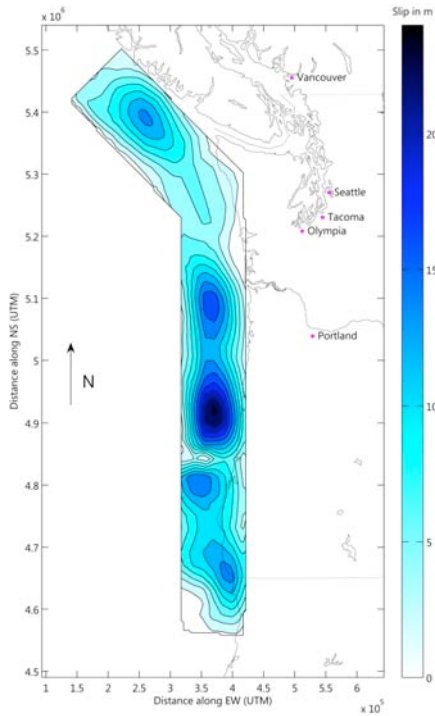


Figure 5. Slip distribution #2 used in the Cascadia megathrust scenario simulation.

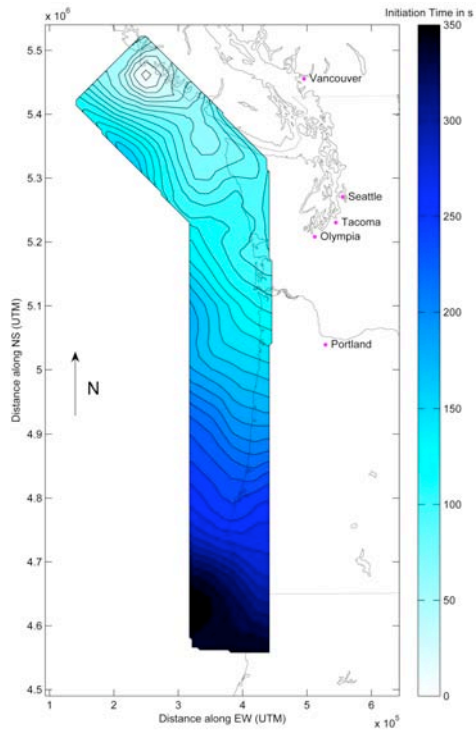


Figure 6. Rupture time distribution #1 used in the Cascadia megathrust scenario simulation.

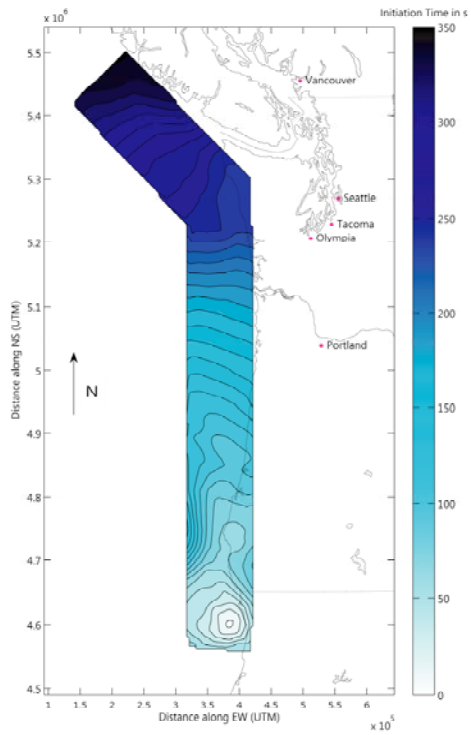


Figure 7. Rupture time distribution #2 used in the Cascadia megathrust scenario simulation.

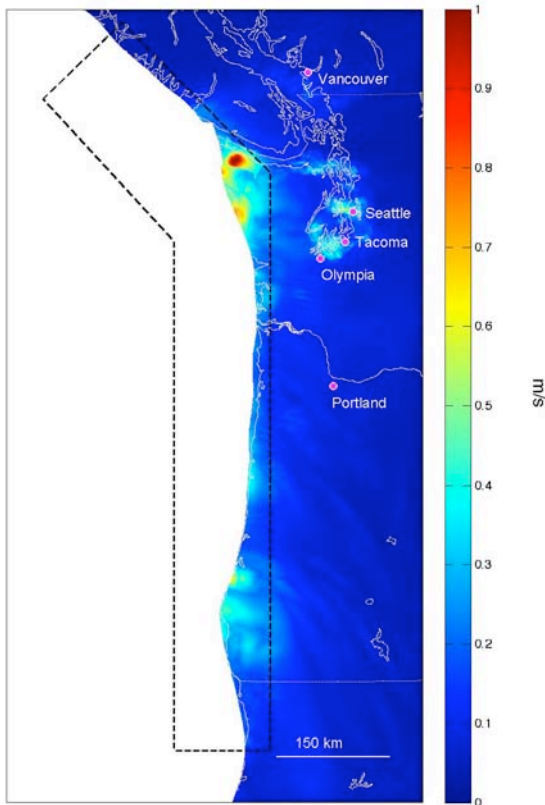


Figure 8. PGVs computed in the Pacific Northwest for M_w 9.0 megathrust earthquake scenario #1. The mean rise time is 32 s, and slip distribution #1 and rupture time distribution #1 (nucleation in the northern end of the rupture zone) are used.

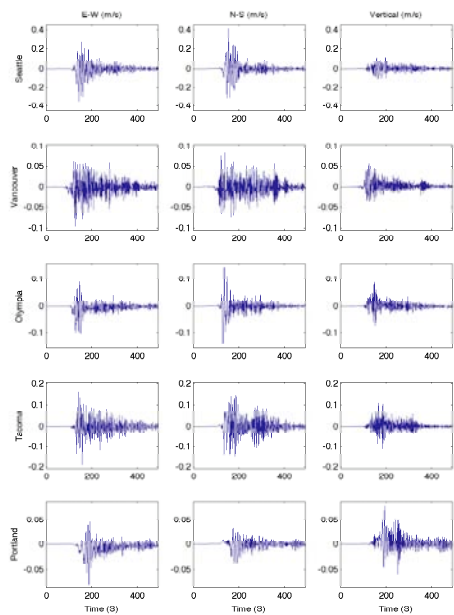


Figure 9. Synthetic seismograms at selected cities in the Pacific Northwest from M_w 9.0 megathrust scenario #1. The mean rise time is

32 s, and slip distribution #1 and rupture time distribution #1 (nucleation in the northern end of the rupture zone) are used.

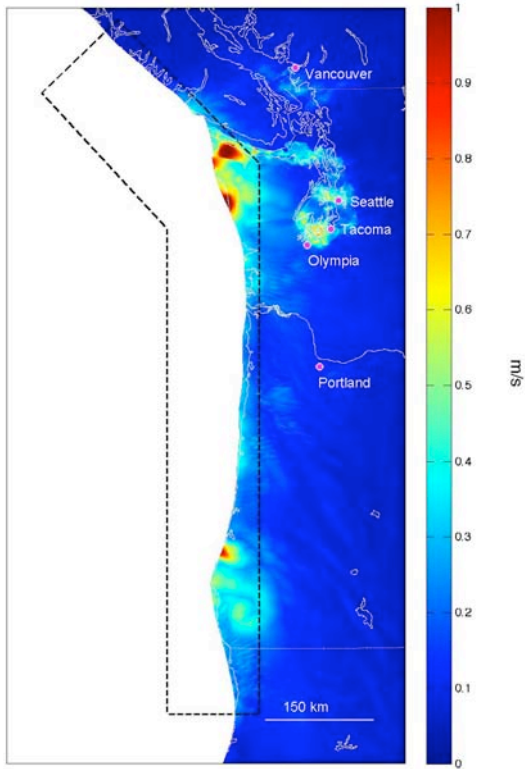


Figure 10. PGVs computed in the Pacific Northwest for $M_w 9.0$ megathrust earthquake scenario #2. The mean rise time is 14 s, and slip distribution #1 and rupture time distribution #1 (rupture nucleation in the northern end of the rupture zone) are used.

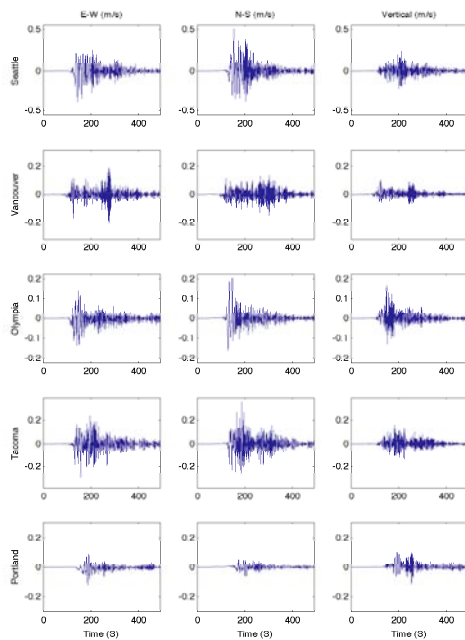


Figure 11. Synthetic seismograms at selected cities in the Pacific Northwest from $M 9.0$ megathrust scenario #2. The mean rise time is 14 s, and slip distribution #1 and rupture time distribution #1 (rupture nucleation in the northern end of the rupture zone) are used.

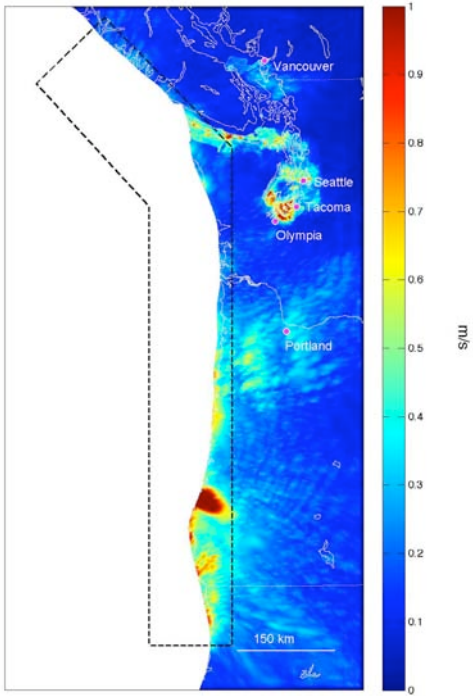


Figure 12. PGVs computed in the Pacific Northwest for $M_w 9.0$ megathrust earthquake scenario #3. The mean rise time is 14 s, and slip distribution #2 and rupture time distribution #1 (rupture nucleation in the northern end of the rupture zone) are used.

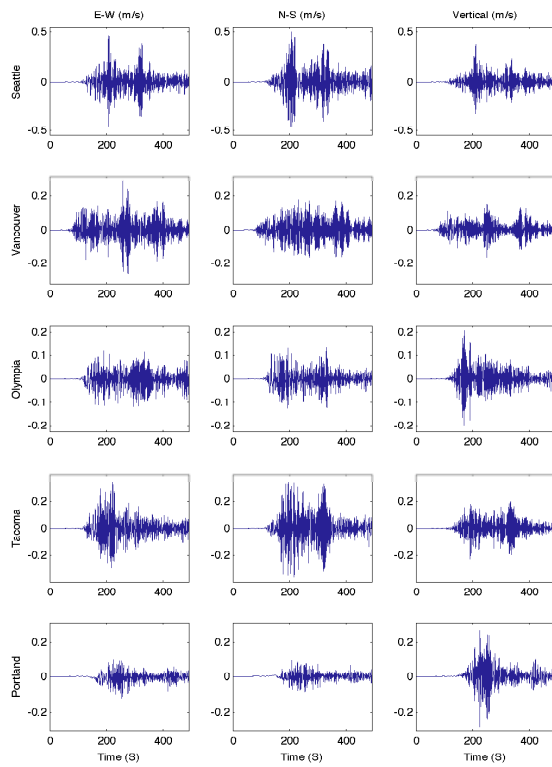


Figure 13. Synthetic seismograms at selected cities in the Pacific Northwest from $M 9.0$ megathrust scenario #3. The mean rise time is 14 s, and slip distribution #2 and rupture time distribution #1 (rupture nucleation in the northern end of the rupture zone) are used.

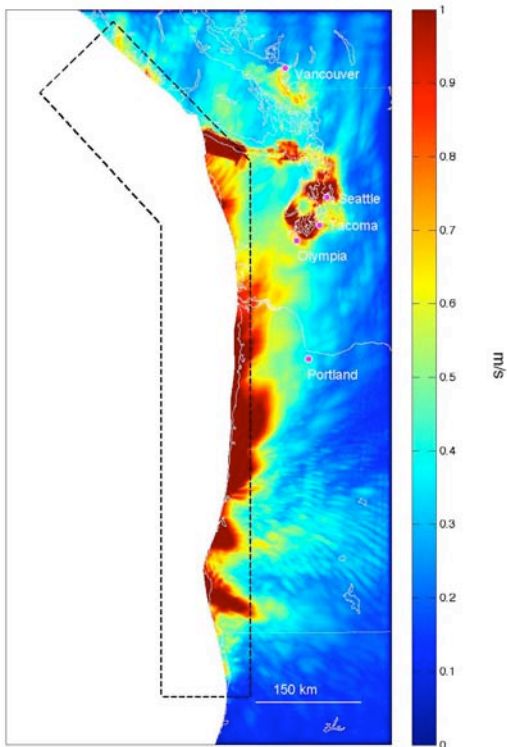


Figure 14. PGVs computed in the Pacific Northwest for M_w 9.0 megathrust earthquake scenario #4. The mean rise time is 14 s, and slip distribution #2 and rupture time distribution #2 (rupture nucleation in the southern end of the rupture zone) are used.

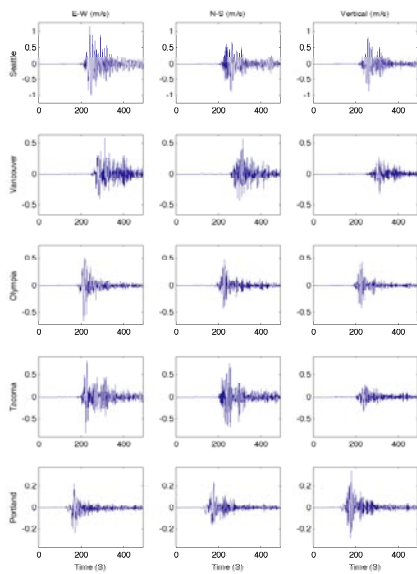


Figure 15. Synthetic seismograms at selected cities in the Pacific Northwest from M 9.0 megathrust scenario #4. The mean rise time is 14 s, and slip distribution #2 and rupture time distribution #2 (rupture nucleation in the southern end of the rupture zone) are used.

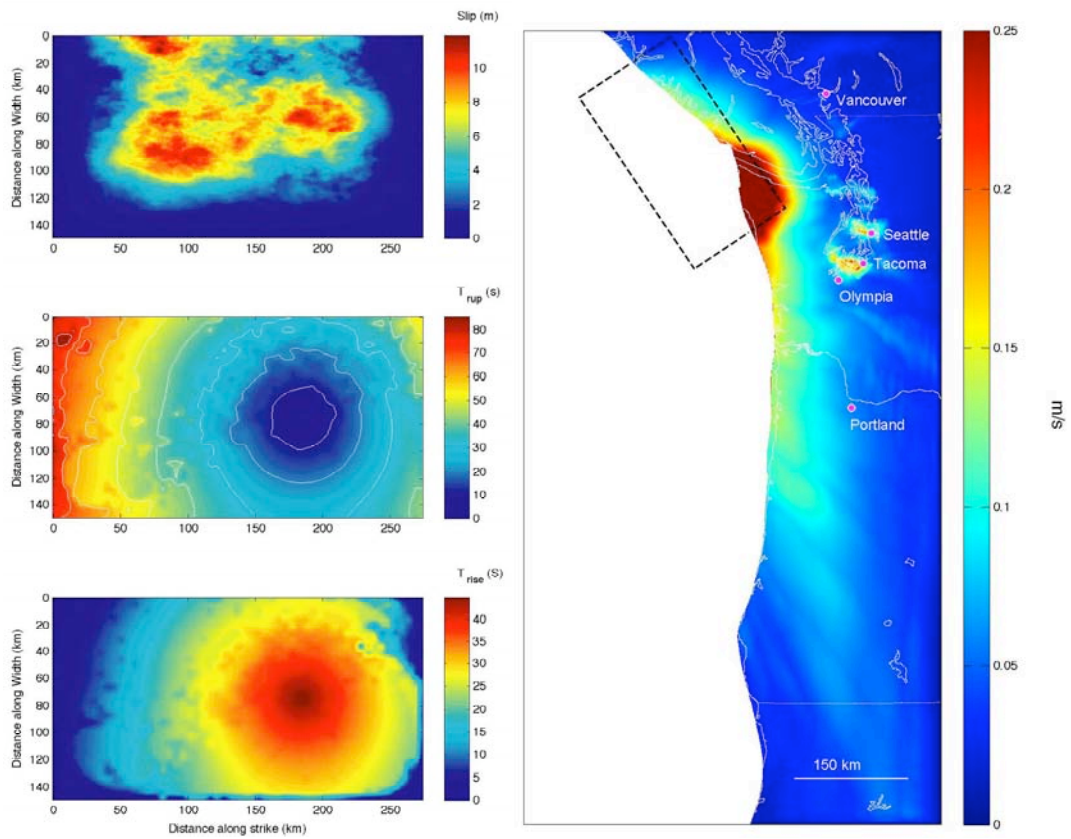


Figure 16. (left) pseudo-dynamic source model and (right) PGVs for Mw 8.5 megathrust earthquake scenario #1. The location of the source is depicted by the dashed rectangle.

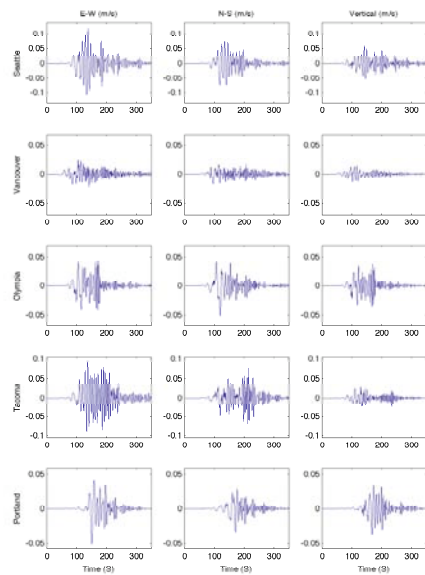


Figure 17. Synthetic seismograms at selected cities in the Pacific Northwest from M8.5 megathrust scenario #1.

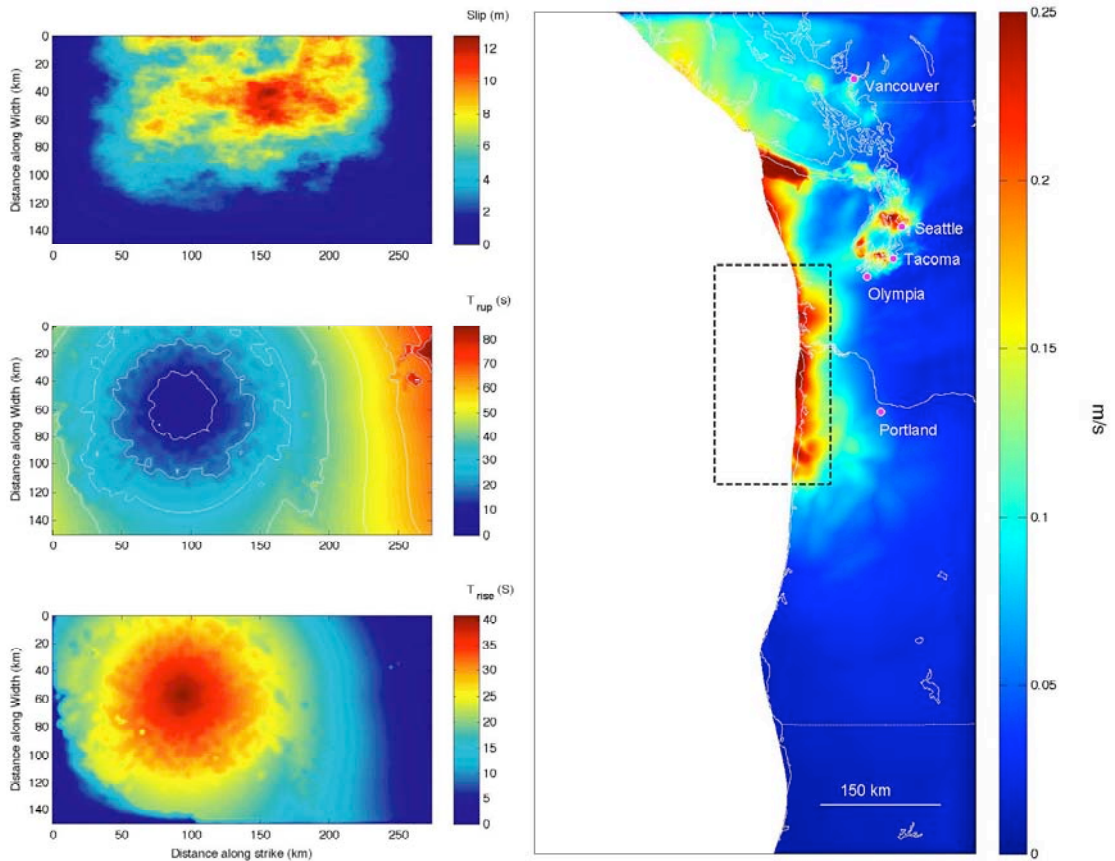


Figure 18. (left) pseudo-dynamic source model and (right) PGVs for Mw 8.5 megathrust earthquake scenario #2. The location of the source is depicted by the dashed rectangle.

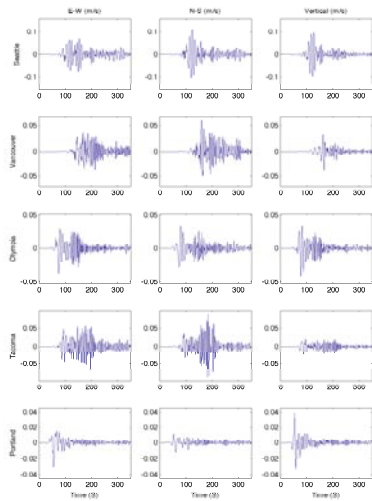


Figure 19. Synthetic seismograms at selected cities in the Pacific Northwest from M8.5 megathrust scenario #2.0